

Laser Beam Defocusing at $1.06\ \mu\text{m}$ by Carrier Excitation in Silicon

Chen Jun and H.-J. Eichler

Optisches Institut, Technische Universität, D-1000 Berlin 12

Received 27 July 1987/Accepted 12 November 1987

Abstract. Laser beams from a 15 ns pulsed Nd:YAG laser are defocused after passing silicon crystals with $400\ \mu\text{m}$ thickness. The beam profile changes into a ring structure at incident laser energies up to 30 mJ and energy densities of $440\ \text{mJ}/\text{cm}^2$. The experimental deflection angles agree with calculations assuming refractive index changes due to electron-hole pairs produced by interband absorption.

PACS: 42.65K, 72.20J, 78.20

Silicon is an effective material for infrared real-time holography with pulsed Nd:YAG-lasers [1] and is also useful for phase conjugation by four-wave mixing [2–4]. In the course of such wave-mixing experiments, it was observed that the transmitted and generated beams change from a Gaussian profile to a ring pattern at high energy densities. In this paper we present a detailed investigation of this defocusing phenomenon using a laser with 15 ns pulse width. Similar observations have been made with picosecond pulses [5].

Experiment

The arrangement is sketched in Fig. 1. A Q-switched Nd:YAG laser beam with 15 ns pulse duration is incident on a silicon slice. The surfaces are antireflection coated with SiO and are set perpendicular to the incident beam. The beam profile has been measured with a detector array (beam probe, Spiricon) and was displayed on a storage oscilloscope.

Figure 2a shows the beam profiles obtained with Q-switched and spiking-mode laser beams passing through the silicon crystals. If the Q-switch is turned off, there is no defocusing and the beam has a Gaussian energy distribution behind the silicon. With the Q-switch operating the laser beam diverges and a ring structure is detected. The appearance of defocusing only for short laser pulses is explained by considering that the carrier lifetime in silicon is between the Q-switched pulse width (15 ns) and the normal mode

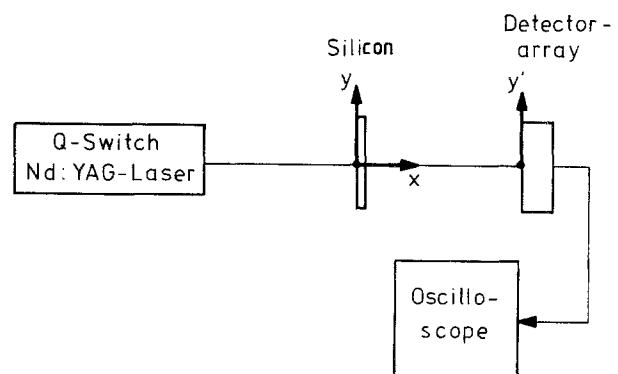


Fig. 1. Experimental arrangement

emission period ($100\ \mu\text{s}$). Therefore with long excitation pulses, the carrier densities and refractive index changes are low.

Figure 2b shows rings with different incident energy densities. The measured ring diameters are given in Table 1 for incident Gaussian beam radii w_0 of 1.3 and 1.9 mm, which are measured by a detector array in the plane of the silicon sample.

We have observed the defocusing effect also in two- and four-wave mixing experiments [3, 4]. Two-wave mixing denotes the coupling and energy exchange between two interfering beams in a nonlinear material. In silicon, the laser-induced dynamic free-carrier grating [6] results in self-diffraction, predominantly of the stronger beam. The diffracted beams have an annular cross-section, if the two incident beams are exactly

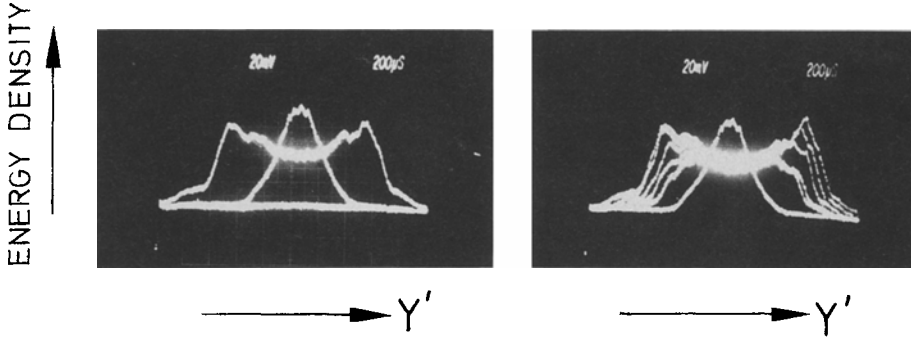


Fig. 2. (a) Laser beam profiles obtained with Q -switched and spiking mode laser beams behind the Si-sample. (b) Ring profiles with different incident energy densities

Table 1. Measured and calculated ring diameters and corresponding path differences for different average energy densities \bar{E} and incident beam radius w_0

\bar{E} [mJ/cm ²]	$w_0 = 1.9$ mm				$w_0 = 1.3$ mm			
	30	43	60	73	140	230	335	440
D_{measured} (mm)	2.8	3.1	3.7	4.1	4.4	5.8	6.6	7
D_{theory} (mm)	2.7	3.0	3.4	3.7	4.6	5.9	7.2	8.2
$\delta n(0,0) \cdot d$	0.5λ	0.7λ	0.9λ	1.1λ	1.8λ	2.7λ	3.4λ	4.0λ

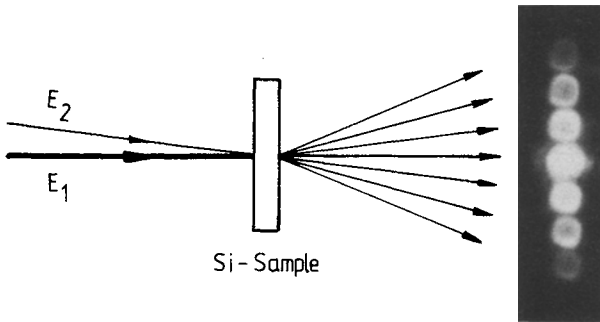


Fig. 3. Defocusing in a two-wave mixing experiment

superimposed (Fig. 3). Otherwise the rings are not perfect and the beam overlap can be controlled thereby. We do not investigate the influence of defocusing on multi-wave mixing further but concentrate on the single beam effect.

Theory

The laser beam with a transversal and temporal intensity distribution $I(y, t)$ is absorbed in the silicon crystal. The induced free carrier density is obtained as [3]

$$N(x, y, t) = \frac{\alpha Q(y, t) \exp(-\alpha x)}{1 + \left(\frac{\sigma}{2}\right) Q(y, t) [1 - \exp(-\alpha x)]} \quad (1)$$

with the integrated photon density

$$Q(y, t) = \frac{1}{h\nu} \int_{-\infty}^t I(y, t') dt' \quad (2)$$

Here x is the distance from the sample surface, α the linear absorption coefficient, σ the electron-hole-pair absorption cross-section, y is a coordinate perpendicular to the propagation direction of the laser beam. Carrier recombination during the laser pulse duration t_p is neglected. The average carrier density leads to a transversal variation of the refractive index

$$\delta n(y, t) = n_{eh} \cdot N(y, t) \quad (3)$$

where

$$\begin{aligned} N(y, t) &= \frac{1}{d} \int_0^d N(x, y, t) dx \\ &= \frac{2}{\sigma d} \ln \left\{ 1 + \frac{\sigma}{2} Q(y, t) [1 - \exp(-\alpha d)] \right\}, \end{aligned} \quad (4)$$

n_{eh} is the change of refractive index produced by one electron hole pair. It should be noted that n_{eh} is negative so that the transversal variation of the refractive index corresponds to a defocusing lens. Figure 4 shows the normalized variation of the refractive index at the pulse center $t=0$ for different energy densities of the total pulse $\bar{E} = h\nu\bar{Q}$. These distributions are nearly Gaussian. The spatially averaged total photon density is defined as

$$\bar{Q} = \frac{0.86}{\pi w_0^2} \int_0^{2\pi} \int_0^{\infty} Q(y, \infty) y dy d\theta.$$

Starting from (3) and the incident laser beam profile, the complex light-field distribution at the exit plane of

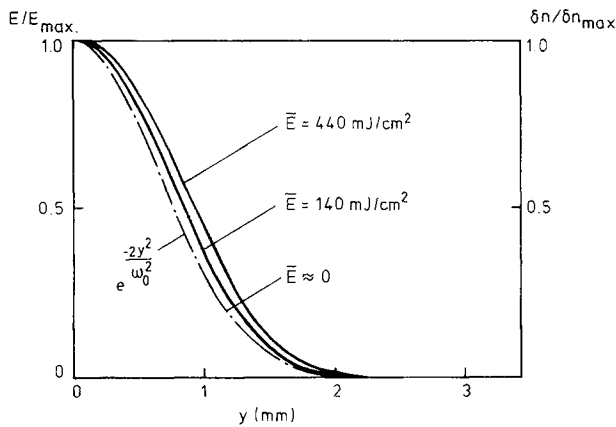


Fig. 4. Normalized variation of the refractive index induced by a Gaussian beam with energy density \bar{E} . Calculated with silicon thickness $d=400 \mu\text{m}$ and beam radius $w_0=1.3 \text{ mm}$

the sample can be calculated. Then a two-dimensional Fourier transform gives the angular distribution of the transmitted laser intensity [7]. In addition, the intensity distribution of the defocused beam has to be integrated temporally to obtain the measured spatial energy distribution. To shorten the mathematics, we do not calculate, in the following, the complete spatial distribution of the defocused beam. Instead an approximation for the ring diameter is obtained by a simplified discussion using geometrical optics. The laser beam is conceived to consist of nearly parallel light rays with a distance y from the beam center. The deflection angle Θ of a light ray passing the silicon sample is given by

$$\Theta(y, t) = \frac{\partial[\delta n(y, t)]}{\partial y} \cdot d. \quad (5)$$

Assuming a Gaussian laser beam

$$Q(y, t) = Q_{\max}(t) \cdot \exp\left(\frac{-2y^2}{w_0^2}\right) \quad (6)$$

the deflection angle is obtained as

$$\Theta(y, t) = \frac{-n_{eh}}{\sigma} \times \frac{AQ_{\max}(t)\sigma \frac{4y}{w_0^2} \exp\left(\frac{-2y^2}{w_0^2}\right)}{1 + \frac{1}{2}AQ_{\max}(t)\sigma \exp\left(\frac{-2y^2}{w_0^2}\right)}. \quad (7)$$

Figure 5 shows the deflection angle $\Theta(y, t=0)$ as a function of y for different average energy densities \bar{E} . For numerical evaluation, the parameters $\alpha=10 \text{ cm}^{-1}$, $\sigma=5 \times 10^{-18} \text{ cm}^2$, $n_{eh}=-9 \times 10^{-22} \text{ cm}^3$ of the silicon crystals were chosen as determined in previous work [1-4] and $A=1-\exp(-\alpha d)$.

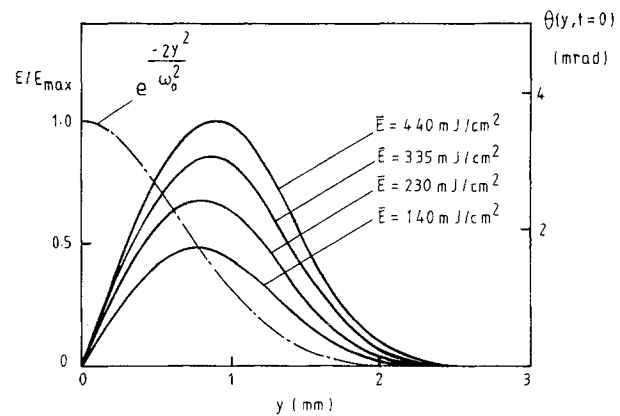


Fig. 5. Gaussian beam profile E/E_{\max} and the deflection angle as a function of y at the pulse center $t=0$ for different energy densities at the total pulse \bar{E}

At the maximum deflection angle $\Theta_{\max}(t)$ the variation of $\Theta(y, t)$ is least. A large part of the beam energy propagates in this direction resulting in a ring structure. The diameter of the ring is given by $\Theta_{\max}(t)$, which increases from the beginning to the end of the laser pulse. Thereby the observed, time integrated ring structure is broadened but not washed out completely. The brightest ring corresponds approximately to the pulse center ($t=0$) where the intensity is maximum. For a symmetrical pulse, an energy density $E_{\max}(0) = \frac{1}{2}E_{\max}(\infty)$ corresponding to half of the total energy has to be considered for evaluation of (7). The ring diameter is then calculated from the distance L between the Si sample and the detector:

$$D = 2\Theta_{\max}(0) \cdot L + D_0, \quad (8)$$

where D_0 denotes the beam diameter calculated at the point of the maximum deflection angle.

Discussion and Summary

Table 1 shows that measured and calculated ring diameters agree reasonably. To obtain a better agreement it seems necessary to calculate the ring diameter more exactly starting from diffraction theory as outlined above.

In the discussion up to now we did not consider thermal refractive index changes and Auger recombination of the carriers, which become important at high energy densities and reduce the defocusing effect. Also the path differences between different points of the exit beam profile are large at high energy densities and the interference between the two regions with the same Θ cannot be neglected. The maximum path differences $\delta n(0, 0) \cdot d$ between the two regions of the beam profile are given in Table 1. For path differences larger than λ

secondary rings are expected due to interference. Experimentally, a second, weak ring is indeed observed in Fig. 2.

Self-focusing or -defocusing are important in the context of photonic switching for the following reasons. First, these effects are present in almost all experiments using optorefractive effects, e.g. four-wave mixing and optical bistability. Second, these effects lead to a convenient method to estimate the nonlinear refractive index changes of photonic materials. The nonlinear refractive index changes can be evaluated from the experimental beam deflection angles. The good agreement between calculated and measured deflection angles (Table 1) proves the validity of the approximation of the theory.

Acknowledgements. This work was supported by the "Deutsche Forschungsgemeinschaft". We thank the IBM Company, Wacker-Chemie-GmbH and Dr. Seifert, Institut für Werkstoffe

der Elektrotechnik, TU Berlin, for the silicon samples, Mr. Gerloff for polishing and Mr. Molt for coating.

References

1. J.P. Woerdman, B. Bölger: *Phys. Lett.* **30A**, 164 (1969)
2. R.K. Jain: *Opt. Eng.* **21**, 199 (1982)
3. H.-J. Eichler, Chen Jun, K. Richter: *Appl. Phys. B* **42**, 215 (1987)
4. H.-J. Eichler, M. Glotz, A. Kummrow, K. Richter, X. Yang: *Phys. Rev.* **35** (to be published)
5. E.W. Van Stryland et al.: In *Picosecond Phenomena III*, ed. by K.B. Eisenthal, R.M. Hochstrasser, W. Kaiser, A. Lauberau, Springer Ser. Chem. Phys. **23** (Springer, Berlin, Heidelberg 1982) p. 368
6. H.-J. Eichler, P. Günter, D.W. Pohl: *Laser-Induced Dynamic Gratings*, Springer Ser. Opt. Sci. **50** (Springer, Berlin, Heidelberg 1986)
7. S.D. Durbin, S.M. Arakelian, Y.R. Shen: *Opt. Lett.* **6**, 411 (1981)